Zirconia and titania nanoparticles studied by electric hyperfine interactions, XRD and TEM

S. Schlabach [a,*], D.V. Szabó [a], D. Vollath [b], P. de la Presa [c], M. Forker [c]

[a] *Institut für Materialforschung III, Forschungszentrum Karlsruhe GmbH, P.O. Box 3640, D-76021 Karlsruhe, Germany*
[b] *NanoConsulting, Primelweg 3, D-76297 Stutensee, Germany*
[c] *Helmholtz Institut für Strahlen- und Kernphysik, University of Bonn, Nussallee 14-16, D-53115 Bonn, Germany*

Abstract

Nanocrystalline ZrO_2 and TiO_2 (n-ZrO_2, n-TiO_2), synthesized in a microwave plasma, have been investigated by X-ray and electron diffraction and by perturbed angular correlation (PAC) measurements of the nuclear electric quadrupole interaction (QI) of the probe nucleus [181]Ta residing on the cation site. The microwave synthesis produces zirconia in the cubic/tetragonal phase, titania in the anatase structure. Grain growth and phase transformations have been studied in bare and Al_2O_3-coated zirconia particles. Coating the nanoparticles with an *amorphous* Al_2O_3 layer obstructs grain growth and may suppress the monoclinic phase.

Keywords: Nanostructures; Crystal structure and symmetry; Scanning and transmission microscopy

1. Introduction

The interaction between a nuclear electric quadrupole moment Q and the tensor of the electric-field gradient (EFG) at the nuclear site is determined by the charge distribution surrounding the probe nucleus. Because of the r^{-3}-dependence of the EFG the main contributions come from the nearest neighbor charges. Strength and symmetry of the nuclear electric quadrupole interaction (QI) therefore provides information on the structure of the solid on a nanometer scale and complements the structural information on nanoscaled solids obtained from X-ray and electron diffraction. We are presently engaged in a program in which structure, grain growth and phase transformations of nanocrystalline (n) ceramics are investigated by perturbed angular correlation (PAC) measurements [1] of electric quadrupole interactions, X-ray diffraction and transmission electron microscopy. In this contribution, we present some results for n-ZrO_2 and n-TiO_2.

2. Experimental

Nanosized samples of bare ZrO_2 and TiO_2 (n-ZrO_2, n-TiO_2) as well as Al_2O_3-coated n-ZrO_2 and n-TiO_2 with sizes typically <5 nm were synthesized

* Corresponding author. Tel.: +49 7247 824471; fax: +49 7247 823956.
E-mail address: sabine.schlabach@imf.fzk.de (S. Schlabach).

using the Karlsruhe microwave plasma process (KMPP). This process is a gas phase process capable of producing bare and coated particles [2,3] with a narrow particle size distribution [4]. Using a microwave plasma discharge and an Ar/20 vol.%O_2 gas mixture as reaction gas, evaporated water free precursors (Ti(OC_4H_9)$_4$, Zr(OC_4H_9)$_4$, $AlCl_3$) react to nanosized oxides at $T \leq 900$ K. The relatively low temperatures avoid sintering of the particles and the evolution of hard agglomerates. The coating of single particles is realized by using two plasma stages consecutively in a closed system. The synthesized powders are collected by thermophoresis.

The particles were characterized in the as-synthesized state by X-ray diffraction (XRD) and transmission electron microscopy (TEM) (Figs. 1 and 2). XRD was carried out with a Philips (X'Pert) diffractometer using Cu Kα radiation at 50 kV and 40 mA on non-compacted powder samples. Grain growth and phase evolution were studied by room temperature XRD measurements of powders annealed in air for 6 h at different temperatures (Fig. 3).

Electron microscope and electron diffraction patterns of powder samples on holey carbon copper grids were recorded with a Philips (CM-30 ST or Tecnai F20 ST) transmission electron microscope.

The PAC measurements were carried out with the 133–482 keV cascade of [181]Ta which is populated in the β$^-$ decay of the 45d isotope [181]Hf. In the synthesis the nanoparticles were doped with the stable isotope [180]Hf by adding about 4 at.% of the corresponding Hf precursor. For the generation of the [181]Hf/[181]Ta probe nuclei, non-compacted powder was enclosed under vacuum into quartz tubes and irradiated in a flux of thermal neutrons of 5×10^{13} n/(s cm^2) for times of the order of 24 h. The PAC spectra were taken with a standard four-detector setup equipped with fast BaF_2 scintillators as a function of temperature in the range 290 K $\leq T_M \leq$ 1500 K. In the study reported here, the samples were cycled between room-temperature and increasing values of T_M. In Fig. 4, the room temperature PAC spectra of [181]Ta in coarse grained ZrO_2 and TiO_2 are compared to those of bare and coated nano-oxides. Fig. 5 illustrates the thermal evolution of the PAC spectra, using n-ZrO_2 and n-ZrO_2/Al_2O_3 as examples.
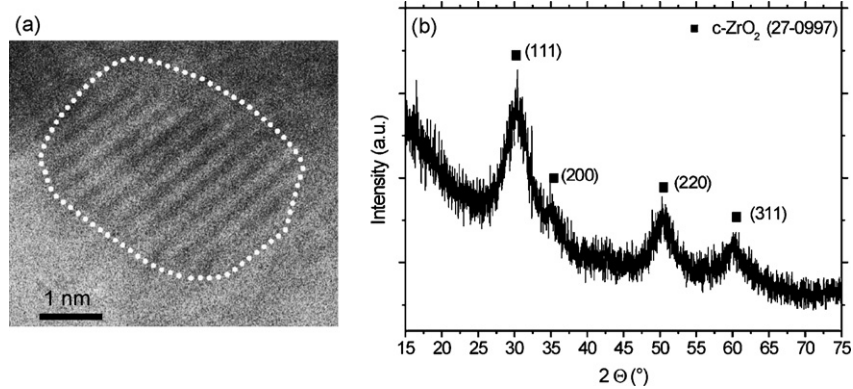
Fig. 1. Electron micrograph (a) and X-ray diffraction (b) of bare n-ZrO$_2$. For comparison $h\,k\,l$-values of c-ZrO$_2$ (JCPDS card no. 27-0997) are given in (b).
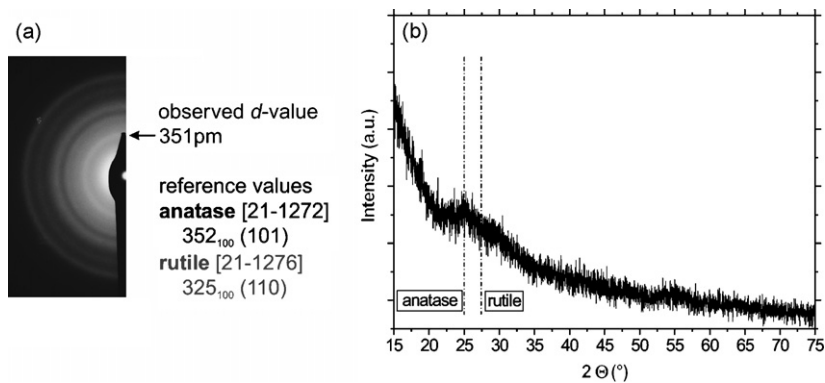

Fig. 2. Electron diffraction (a) and X-ray diffraction (b) of bare n-TiO$_2$. For comparison d-values of reference anatase (JCPDS card no. 21-1272) and rutile (JCPDS card no. 21–1276) structure are given.

3. Results and discussion

The electron and X-ray diffraction data (Figs. 1 and 2) clearly show that the structure of the as-synthesized powders differs from that usually observed in the bulk material at room temperature: n-ZrO$_2$ is in the cubic or tetragonal rather than the monoclinic phase, n-TiO$_2$ has the anatase rather than the rutile structure. This reverse phase stability at very small particle sizes is described by several authors [for TiO$_2$ see e.g. 5–7]. It can be attributed to the fact that the possible phases differ in the surface contribution to the free energy. As the relative surface
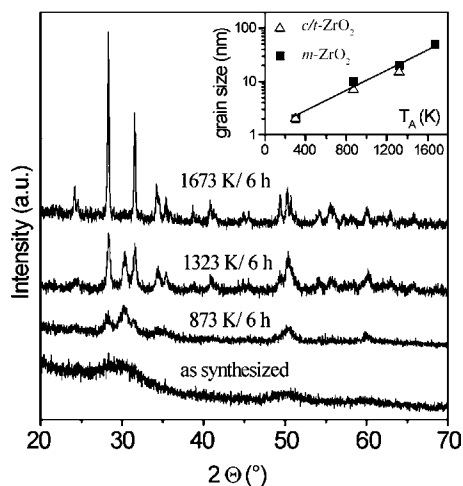

Fig. 3. Room temperature X-ray diffraction pattern of n-ZrO$_2$ as synthesized and after annealing for 6 h at the temperatures given. The insert shows the grain size as a function of the annealing temperature.
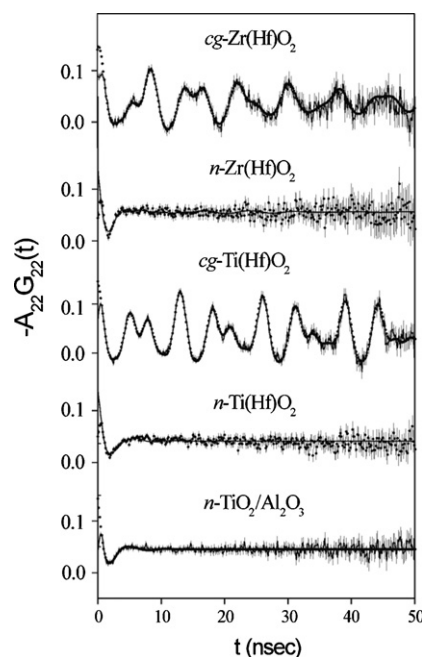

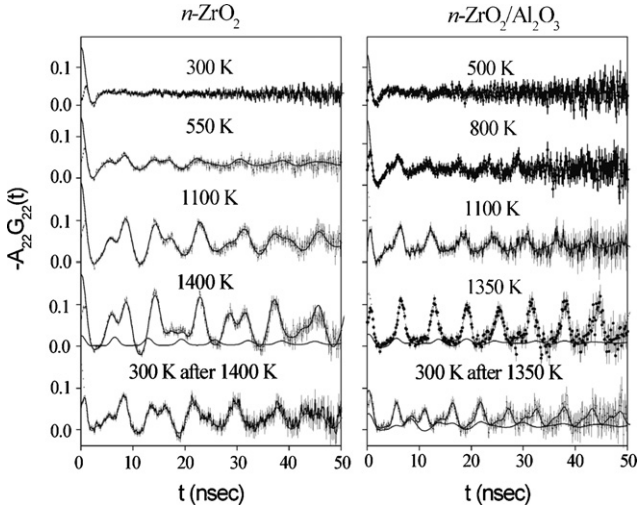Fig. 4. ^{181}Ta PAC spectra in coarse-grained (cg-) and nanocrystalline n-ZrO$_2$ and n-TiO$_2$ at 300 K.

Fig. 5. PAC spectra of [181]Ta in bare and Al₂O₃-coated ZrO₂ nanoparticles at different temperatures.

part increases with decreasing particle size, the phase stability in the nm-range may differ from that of the coarse grained (cg-) material [see e.g. 8,9]. In the TEM micrographs which basically reflect the cation sub-lattice, one recognizes a fairly well established long range order. Fig. 3 illustrates the changes of the XRD spectra of n-ZrO₂ upon annealing. The annealing process leads to (i) the transformation of the initially c/t-phase to monoclinic ZrO₂ and (ii) to grain growth, shown by the decrease of the line width of the X-ray peaks with increasing annealing temperature T_A. The insert shows the grain size determined from the line width using the Scherrer-formula [10]. The exponential increase of the grain size with increasing T_A corresponds to a grain growth activation enthalpy of $Q_A \sim 30$ kJ/mol, in fair agreement with the result of Siu et al. [11] for n-ZrO₂ prepared by the hydrothermal method. Similar annealing experiments for Al₂O₃-coated ZrO₂ and n-TiO₂ are under way.

In Fig. 4 we compare the [181]Ta PAC spectra of n-ZrO₂, bare and Al₂O₃-coated n-TiO₂ to those of the corresponding coarse-grained material. In the case of cg-ZrO₂ and cg-TiO₂ the time spectrum of the anisotropy shows the well-known non-periodic oscillatory structure typical for the axially asymmetric QI of m-ZrO₂ [12] and rutile TiO₂ [13], respectively. In the nanocrystalline powders, however, the oscillations of the anisotropy are completely wiped out. This is a clear indication that the probe nuclei no longer experience a single well-defined electric field gradient (EFG), but are subject to a broad distribution of different QI's. Because of the r^{-3} dependence of the EFG, the measurements of the QI mainly sample the charge distribution of the nearest-neighbor environment of the probe nucleus. In ZrO₂ and TiO₂, oxygen ions are the nearest neighbors of the metal sites. The broad QI distribution seen by [181]Ta on the Zr- or Ti-site therefore implies a high degree of disorder of the oxygen sublattice which contrasts with the long-range order of the cation sublattice seen in TEM micrographs.

Upon annealing, the broad QI distribution characteristic for the nanoparticles in the as-synthesized state evolves towards to a well defined QI. This gradual transition is illustrated in Fig. 5 for n-ZrO₂ and n-ZrO₂/Al₂O₃. In bare n-ZrO₂, one first finds the
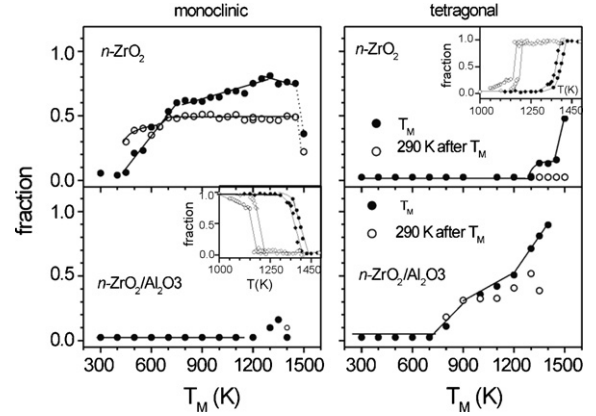

Fig. 6. The thermal evolution of the monoclinic and the tetragonal phase in bare and Al₂O₃-coated ZrO₂ nanoparticles, observed by [181]Ta PAC spectroscopy. The inserts show the m ↔ t transitions of bulk ZrO₂.

non-periodic oscillation of monoclinic ZrO₂ and an admixture of the periodic pattern of tetragonal ZrO₂ is observed only at $T \geq 1400$ K. In coated n-ZrO₂/Al₂O₃, it is the tetragonal phase which first appears upon heating, the monoclinic phase is suppressed practically up to $T \sim 1350$ K. The relative intensities of the monoclinic and the tetragonal phase in the spectra of Fig. 5 have been extracted using standard PAC analysis. The results are collected in Fig. 6 and compared (see inserts) to the phase transformations in the bulk material. In non-coated n-ZrO₂ the monoclinic phase develops gradually. The transformation to the tetragonal phase occurs at about the same temperature and is as sharp as in cg-ZrO₂. An interesting result which asks for further investigation is the observation that upon cooling to 300 K the relative intensity of the monoclinic phase is significantly reduced. This reduction implies that at 300 K a part of the probe nuclei is subject to another unresolved high frequency QI. The fact that this reduction does not occur in the bulk material suggests a relation of this phenomenon to the interfacial region of the nanoparticles.

A comparison between the PAC spectra of [181]Ta in n-ZrO₂ and n-ZrO₂/Al₂O₃ (Fig. 5) and the corresponding relative phase intensities (Fig. 6) clearly shows that a coating of the particles with amorphous Al₂O₃ strongly affects the phase transformations in nanocrystalline zirconia. In contrast to non-coated zirconia, at $T > 700$ K the content of tetragonal ZrO₂ increases continuously, while the monoclinic phase is almost entirely suppressed. The difference can be attributed to the volume expansion of $\sim 4.5\%$, which accompanies the tetragonal-monoclinic transformation in zirconia. In particles mechanically confined by an Al₂O₃ coating, this expansion leads to compressive stresses which stabilize the tetragonal phase. Akin to the obstructed phase transformations, the grain growth of the coated particles is hindered, too. The coated material exhibits $\sim 40\%$ of the particle size of theirs uncoated counterparts after annealing under similar conditions.

4. Conclusion

The combination of electron and X-ray diffraction with measurements of electric quadrupole interactions allows comple-

mentary insights into structure, phase transition and grain growth of ceramic nanoparticles as zirconia, titania and others. The diffraction methods reflect the degree of long-range order of the cation sublattice, the electric quadrupole interaction samples the charge distribution surrounding the metal sites and therefore provides information on the order of the oxygen sublattice.

The microwave plasma synthesis of ZrO_2 and TiO_2 leads to the cubic/tetragonal and the anatase rather the monoclinic and rutile structure, respectively, usually found in the coarse-grained oxides. With increasing temperature, grain growth and phase transformations have been observed. For n-ZrO_2 the grain growth activation enthalpy has been determined. Coating the particles with amorphous Al_2O_3, suppresses the monoclinic phase in zirconia and also obstructs grain growth.

Acknowledgements

References

[1] G. Schatz, A. Weidinger, Nuclear Solid State Physics, Wiley, New York, 1996.
[2] D. Vollath, K.E. Sickafus, Nanostruct. Mater. 1 (1992) 427–437.
[3] D. Vollath, D.V. Szabo, Nanostruct. Mater. 4 (1994) 927–938.
[4] D. Vollath, D.V. Szabó, in: K.L. Choy (Ed.), Innovative Processing of Films and Nanocrystalline Powders, Imperial College Press, London, 2002, pp. 219–251.
[5] Y. Hu, H.-L. Tsai, C.-L. Huang, Mater. Sci. Eng. A 344 (2003) 209–214.
[6] V. Swamy, A. Kuznetsov, L.S. Dubrovinsky, R.A. Caruso, D.G. Shchukin, B.C. Muddle, Phys. Rev. B 71 (2005) 184302_1–184302_11.
[7] K.-R. Zhu, M.-S. Zhang, J.-M. Hong, Z. Yin, Mater. Sci. Eng. A 403 (2005) 87–93.
[8] H. Zhang, J.F. Banfield, J. Mater. Chem. 8 (1998) 2073–2076.
[9] R.C. Garvie, M.F. Goss, J. Mater. Sci. 21 (1986) 1253–1257.
[10] H.P. Klug, L.E. Alexander, X-ray Diffraction Procedures, 2nd ed., Wiley, New York, 1974.
[11] G.G. Siu, M.J. Stokes, Y. Liu, Phys. Rev. B 59 (1999) 3173–3179.
[12] H. Jaeger, J.A. Gardener, J.C. Haygarth, R.L. Rasera, J. Am. Ceram. Soc. 69 (1986) 458–463.
[13] J.M. Adams, G.L. Catchen, Phys. Rev. B 50 (1994) 1264–1267.